Volume 56
Number 83
25 October 2020
Pages 12449–12672

ChemComm

Chemical Communications

rsc.li/chemcomm

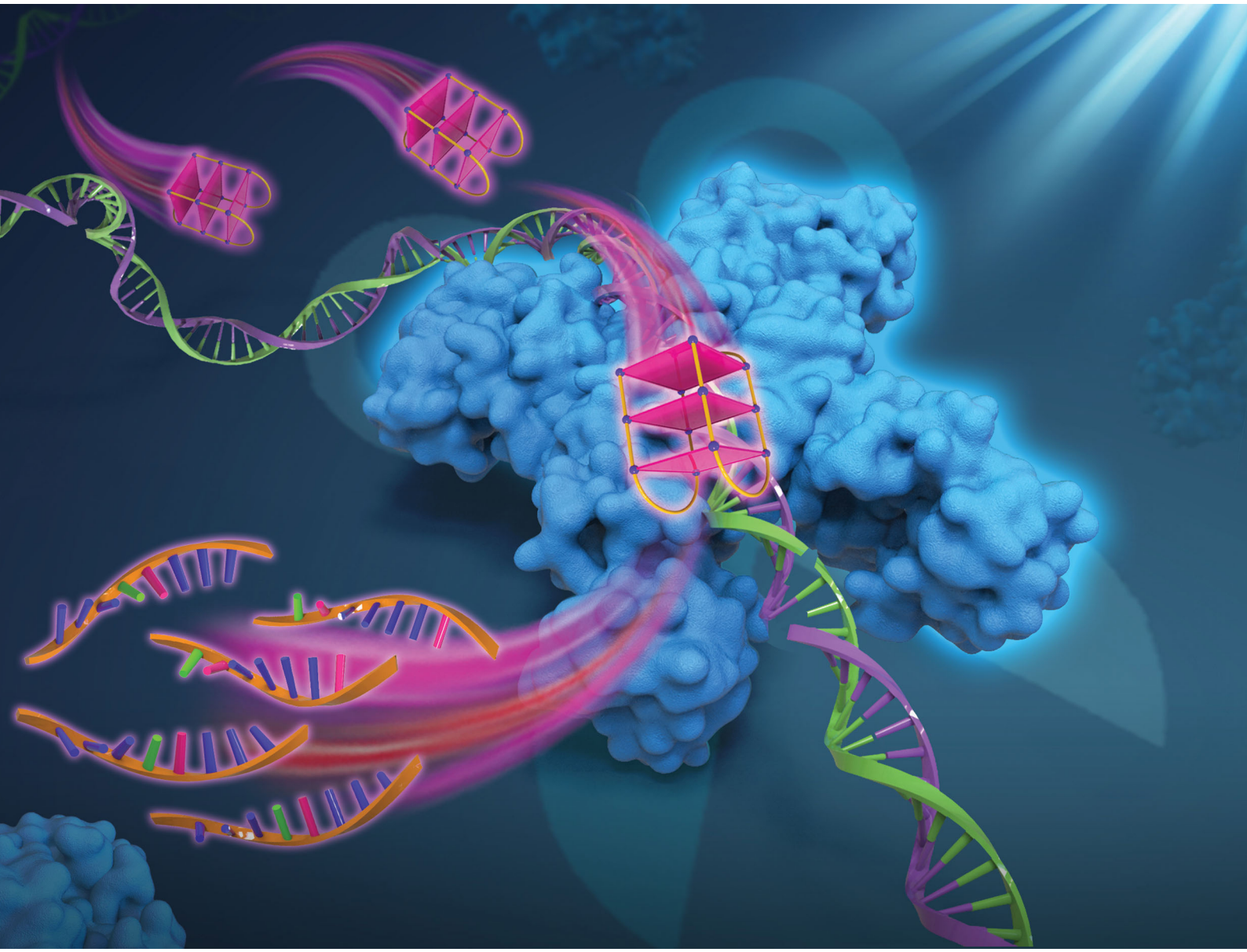

ISSN 1359-7345

ROYAL SOCIETY OF CHEMISTRY

COMMUNICATION

Ying Li, Maili Liu *et al.*

CRISPR-Cas12a *trans*-cleaves DNA G-quadruplexes

ChemComm

COMMUNICATION

View Article Online
View Journal | View Issue

Cite this: *Chem. Commun.*, 2020, **56**, 12526

Received 14th August 2020,
Accepted 13th September 2020

DOI: 10.1039/d0cc05540a

rsc.li/chemcomm

CRISPR-Cas12a *trans*-cleaves DNA G-quadruplexes†

Ying Li, ‡*[ab] Tao Li,‡[ab] Bi-Feng Liu,[c] Rui Hu,[ab] Jiang Zhu,[a] Ting He,[a] Xin Zhou,[ab] Conggang Li,[ab] Yunhuang Yang[ab] and Maili Liu*[ab]

We for the first time report that the activated CRISPR-Cas12a system *trans*-cleaves DNA G-quadruplexes (G4). The cleavage activity on human telomere G4 and TBA G4 was investigated and verified by FRET, CD, gel electrophoresis and NMR. We believe that this finding will pave a new avenue for advancing the applications of CRISPR-Cas12a and G4 in biosensing and biochemistry.

CRISPR-Cas12a (also known as Cpf1) proteins are RNA-guided enzymes that bind single-stranded DNA (ssDNA) or double-stranded DNA (dsDNA) and cleave the target DNA, and serve as components of bacterial adaptive immune systems.[1–3] The CRISPR RNA (crRNA) guided precision cleavage of the targets makes the system a promising tool for gene-editing applications.[4] Recently, it has been found that the activated CRISPR-Cas12a system has a collateral effect of promiscuous endonuclease activity on non-target ssDNA (*trans*-cleavage) besides its capability of cutting the target DNA (*cis*-cleavage).[5,6] This finding inspired the community to develop promising biosensors for fast and sensitive detection of viruses and other biospecimens.[5,7,8] When we were trying to develop a CRISPR-Cas12a based biosensor for the detection of SARS-CoV-2, we surprisingly found that the activated *Lachnospiraceae* bacterium ND2006 Cas12a (LbCas12a) also has *trans*-cleavage activity on DNA G-quadruplexes (G4).

Guanine-rich DNA sequences can fold into four-stranded, noncanonical secondary structures termed G4s through Hoogsteen hydrogen bonds.[9] We labelled the human telomeric G4 sequence ($(TTAGGG)_4$) at the 5′ and 3′ end with FAM and TAMRA, respectively. The strong fluorescence resonance energy transfer (FRET) signal between the two probes suggested that the sequence formed a higher-order structure in LbCas12a buffer (50 mM NaCl, 10 mM Tris–HCl, 10 mM $MgCl_2$, pH7.9) (Fig. S1a, ESI†).[10] The circular dichroism (CD) data demonstrated that it formed an antiparallel G4 structure (Fig. S1b, ESI†).[11] We then used SARS-CoV-2 N-gene as the target sequence (termed as target sample) and SARS N-gene as a non-target control. After the assembly of the LbCas12a/crRNA complex, the addition of the SARS-CoV-2 N-gene activated the cleavage activity on the G4 structure, which resulted in the separation of the two fluorophore probes and induced a dramatic decrease of the FRET efficiency (Fig. 1a). For the SARS N-gene, it could not activate the LbCas12a/crRNA complex and the G4 structure remained intact, which showed the same FRET efficiency as that under ''Buffer'' conditions (blank control) without any gene sequence. Then we used a CD spectrometer to examine the degradation of the G4 structure. As shown in Fig. 1b, the spectra of the two controls kept the features of a typical antiparallel G4 (a positive peak at 295 nm and a negative peak at 265 nm),[12] while the specific peaks changed dramatically for the target sample, indicating a disruption of the G4. Furthermore, we used agarose gel electrophoresis to prove the cleavage. Fig. 1c demonstrated that the cleaved G4 sequence in the target sample displayed multiple bands with small molecular weights (the 4th lane), while the other two controls (the 2nd and 3rd lane) displayed a single band. In addition, we also added another buffer condition (without Na^+, the 5th lane) as a control, where the telomere G4 sequence should present as a linear oligonucleotide.[13]

Moreover, the *trans*-cleavage of activated LbCas12a on 100 mM Na^+-induced G4 was further validated using ^1H NMR spectroscopy. As shown in Fig. 1d, the resonances between 10 and 12 ppm revealed the formation of G4 structures (top panel)[11,14] and

[a] *State Key Laboratory of Magnetic Resonance and Atomic Molecular Physics, Wuhan National Laboratory for Optoelectronics, National Centre for Magnetic Resonance in Wuhan, Wuhan Institute of Physics and Mathematics, Innovation Academy for Precision Measurement Science and Technology, Chinese Academy of Sciences – Wuhan National Laboratory for Optoelectronics, Huazhong University of Science and Technology, Wuhan, 430071, China. E-mail: liying@wipm.ac.cn, ml.liu@wipm.ac.cn*

[b] *University of Chinese Academy of Sciences, Beijing, 10049, China*

[c] *The Key Laboratory for Biomedical Photonics of MOE at Wuhan National Laboratory for Optoelectronics – Hubei Bioinformatics & Molecular Imaging Key Laboratory, Systems Biology Theme, Department of Biomedical Engineering, College of Life Science and Technology, Huazhong University of Science and Technology, Wuhan, 430074, China*

† Electronic supplementary information (ESI) available. See DOI: 10.1039/d0cc05540a

‡ These authors contributed equally to this work.

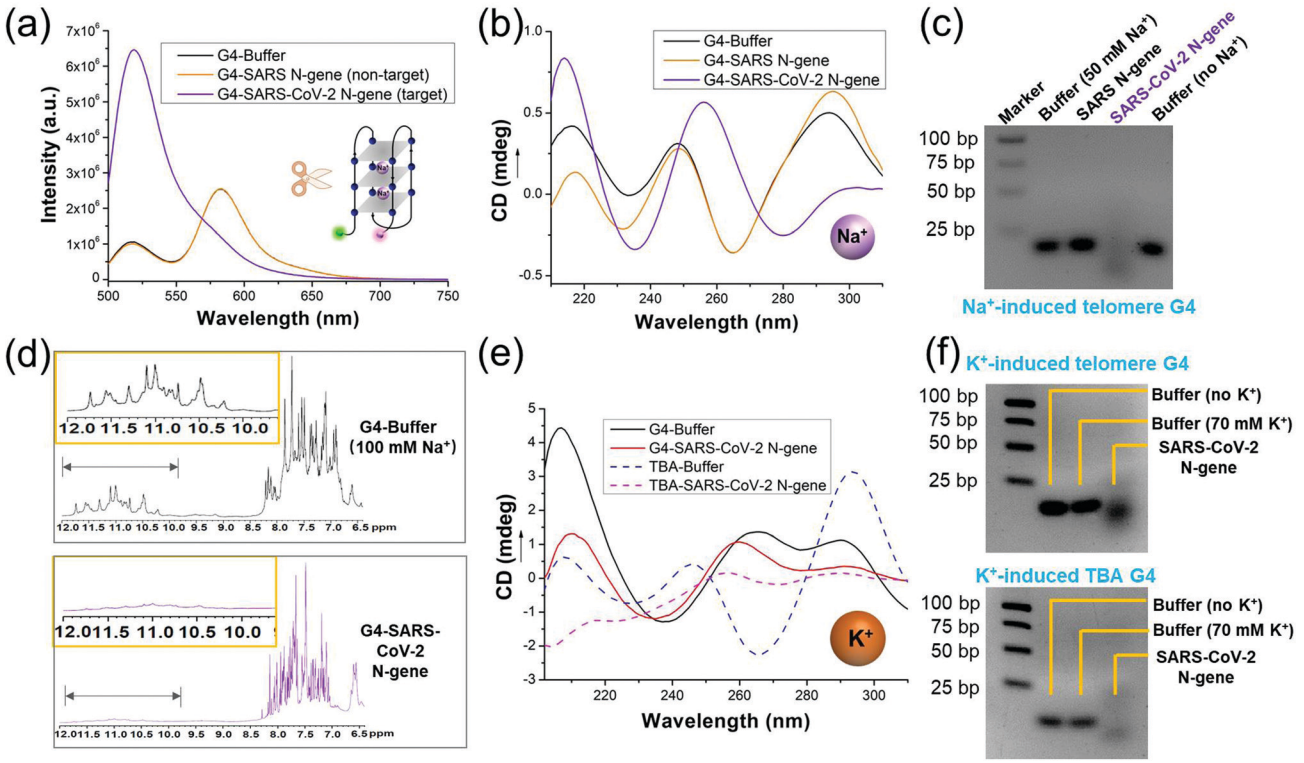

Fig. 1 The *trans*-cleavage of activated CRISPR-Cas12a on various G4 structures. (a–d) Investigation of LbCas12a *trans*-cleavage on Na^+-induced telomere G4 by FRET (a), CD (b), agarose gel electrophoresis (c) and ^1H NMR (d). (e and f) Results of CD (e) and agarose gel electrophoresis (f) showing LbCas12a *trans*-cleavage on K^+-induced telomere G4 and TBA G4.

the disappeared peaks in this range (bottom panel) proved the G4 degradation after the cleavage. In addition, the sharper and narrower resonances for the base protons resonating between 7.0 and 8.5 ppm of the cleaved sample demonstrated that there were smaller elements produced in comparison to the non-cleaved sample. Taken together, we here show that the LbCas12a system can be specifically activated by the target gene and trans cleaves the Na^+-induced telomere G4 structure.

We wondered if this *trans*-cleavage on G4 also worked for other G4s, such as K^+-induced telomere G4 with a parallel/antiparallel hybrid structure[13,15] and K^+-induced TBA (thrombin binding aptamer)[16,17] with an antiparallel structure. We then used FRET, CD and gel electrophoresis to check the cleavage activity. The results in Fig. 1e and Fig. S2 (ESI†) indicated the formation of telomere G4[15,18] and TBA G4.[16,17] The changes of the fluorescence spectra in Fig. S2 (ESI†), CD spectra in Fig. 1e and the multiple bands of the target sample in Fig. 1f proved the cleavage on the two types of G4s. These data demonstrated that the LbCas12a system can *trans*-cleave different types of G4s.

Following the above finding, we then performed more tests to further investigate the cleavage activity of an LbCas12a system on Na^+-induced G4. First, we tested whether the target concentration could affect the cleavage efficiency. The fluorescence spectra were acquired after 15 min cleavage under 37 °C. The results in Fig. 2a demonstrated that the FRET efficiency decreased correlated with the target-gene concentration and the 0.02 nM target sample could be clearly distinguished from the buffer. This result revealed that the combination of CRISPR-Cas12a and G4 holds great potential for biosensing applications if integrating some DNA pre-amplification strategies.[5,7] Then we interrogated the *trans*-cleavage kinetics of the system on 50 mM Na^+-induced G4. The time course fluorescence spectra in Fig. 2b demonstrated the on-going cleavage progress (at 37 °C). The cleavage was almost accomplished in about 30 min, indicated by the disappeared peak at ~583 nm.

Next, we increased the Na^+ concentration to examine whether it could affect the cleavage kinetics of LbCas12a. Surprisingly, we found that the cleavage speed on the G4 structure was much slower in the higher Na^+ solution (Fig. 2c), especially for the condition with 200 mM Na^+. The time to fully cut the G4s required 0.5 h, >1 h, >4 h and >40 h for 50 mM, 100 mM, 150 mM and 200 mM Na^+, respectively (Fig. S3, ESI†). These results suggested that the cleavage of the LbCas12a system on the G4 structures might depend on G4's stability since higher-Na^+ solution induces the formation of a more stable G4.[18] We further studied the kinetics of the cleavage system on a K^+-induced G4 structure. Potassium is reported to promote the formation of G4 that is recognized as relatively more stable than that induced by Na^+.[19,20] However, we were still surprised to find that it required so long a time (up to 14 hours) to fully cleave the 70 mM K^+-induced G4 (Fig. S4, ESI†). The cleavage speed is much slower than that of

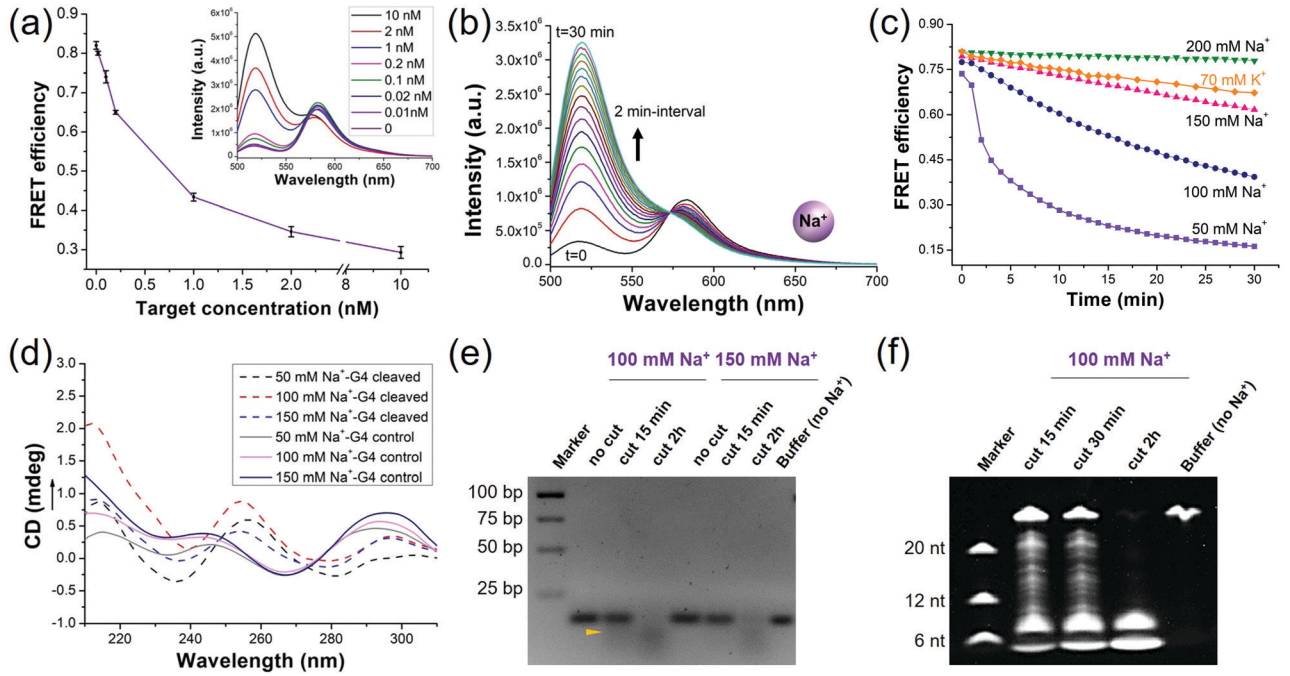

Fig. 2 *trans*-Cleavage kinetics of LbCas12a on telomere G4. (a) Changes of the FRET efficiency against the target DNA with various concentrations (spectra shown as the inset). Error bars represent the average of the FRET efficiency of three measurements for the sample. (b) Time course cleavage on 50 mM Na^+-induced G4. (c) Cleavage kinetics of various Na^+ solutions and 70 mM K^+-induced G4. (d) CD spectra of the G4s before and after trans cleavage. (e) Products at different time points of cleavage on 100 mM- and 150 mM-Na^+ induced G4 resolved by agarose gel electrophoresis (e) or denaturing PAGE (f). The yellow arrow in (e) indicates the degraded sequences.

100 mM Na^+, and between those of 150 mM and 200 mM Na^+ (Fig. 2c). We wondered about the possibility that K^+ could inhibit the enzyme activity of LbCas12a and hence influence the cleavage efficiency. We then tested the cleavage efficiency of LbCas12a on an ssDNA reporter[5] that should not have a higher-order structure under different ion conditions. As shown in Fig. S5 (ESI†), K^+ did not inhibit but even promoted the cleavage efficiency on the ssDNA reporter compared to Na^+, and different Na^+ solutions did not affect the enzyme activity significantly. Therefore, we consider that the differences of cleavage speed between K^+- and Na^+-induced G4s might be explained by using the theory of melting temperature (T_m) since the T_m of G4 has similar variations between K^+- and Na^+-induced structures under similar conditions.[18,20] These data further corroborate that the *trans*-cleavage speed of the LbCas12a system on G4 structures depends on the stability of G4s.

For various concentrations of Na^+-induced G4, the CD data in Fig. 2d demonstrated that the cleaved G4s displayed completely different spectra in comparison to the controls. Then we further used time-lapse CD scanning (at 37 °C) to directly check the cleavage intermediates. To see the changes more apparently, the concentrations of LbCas12a and other reagents were increased (more details are shown in the ESI†). Fig. S6 (ESI†) demonstrated that typical CD peaks for the antiparallel G4 started to change after the cleavage was initiated. The on-going cleavage gradually shifted the relevant peaks and eventually achieved complete cutting. Gel electrophoresis could present intermediate products more straightforward than CD and fluorescence spectra. Fig. 2e demonstrated the cleavage results of the 100 mM and 150 mM Na^+-induced G4 structures. The 15 min cutting generated an intermediate state and the bands at the 3rd lane (100 mM Na^+ sample) clearly suggested that both the G4 structure and degraded sequences existed, consistent with the FRET and CD results (Fig. S3 and S5, ESI†). In comparison to the 5th lane, the 6th lane with a slightly weaker G4 band further suggested the difficulty of cutting 150 mM Na^+-induced G4 in a short time. To see the cleaved products more clearly, we used denaturing polyacrylamide gel electrophoresis (PAGE) based on fluorescence imaging to dissect the cleaved sequences. The results shown in Fig. 2f indicated that, in the cleavage intermediates, the 5′-FAM labelled G4 sequence was cut into many products with various sizes. However, overall it was mainly degraded into two segments with sizes of ~4 nt and ~8 nt, similar to that of *trans*-cleaved products of ssDNA.[6]

Activated CRISPR-Cas12a has recently been found to possess *trans*-cleavage ability to cut non-target ssDNA, but not dsDNA or RNA.[5,6,21] In this work, we for the first time demonstrated that the activated LbCas12a also has the capability to *trans*-cleave different types of DNA G4 structures. This new finding expands the *trans*-cleavage objectives of Cas12a and allows great potential to further extend the function and advance the application of this system. For example, many promising platforms have been developed based on CRISPR-Cas12a for ultrasensitive detection of viruses such as human Papillomavirus, SARS-CoV-2 and others since the finding of the collateral

activity on ssDNA[5,7,22] G4 has been proven to be a highly successful signal transducer due to its sensitive response to various environmental stimuli (*e.g.*, various metal ions, hemin, thioflavin T).[23] Numerous G4-based biosensors have been designed for the detection of various targets.[24,25] By combining CRISPR-Cas12a and G4, we believe that more favorable diagnostic platforms could be designed with high sensitivity and specificity. In addition, if integrated with some pre-amplification strategies (*e.g.*, polymerase chain reaction with 30 cycles),[7,8,26] such systems could achieve a detection sensitivity better than attomole for virus DNA (briefly calculated based on our preliminary data on the detection of SARS-CoV-2 N-gene).

In addition to the above-mentioned potential applications, the *trans*-cleavage mechanism on G4 is also an aspect worthy to investigate. Our experiments about K^+ and various Na^+ induced G4 suggested that the efficiency of the cleavage on G4 is highly related to its stability, which implied that the cleavage mechanism might be different from that on ssDNA.[5] By the way, we found that G-triplexes (G3), another DNA structural motif similar to G4, could also be cleaved by LbCas12a, but it is easier to cleave G3 than G4 under the same conditions probably due to the lower stability of G3 (data not shown).[16,17,27] A possible reason for the relevance of G4 stability and cleavage efficiency could be that the more stable structure might protect some specific cleavage sites better, which thus slows down the *trans*-cleavage. However, more evidence is required to support such a hypothesis. We believe that it is worth putting more effort into the detailed cleavage mechanism on G4 in future. Here we can list a few questions: does the cutting on the G4 sequence occur randomly or is it site-selected? How does the G4 stability affect the cleavage speed? Do Cas12a orthologs from other species also *trans*-cleave DNA G4?[28] Is it possible that these Cas12a orthologs have different cleavage efficiencies on G4 structures?

Like CRISPR-Cas9, CRISPR-Cas12a is also an important adaptive immunity in bacteria and this system has now been widely harnessed for genome editing.[4] Within a host bacterium, the *trans*-cleavage capability on ssDNA was supposed to help the bacteria degrade temporal ssDNA sequences.[3] This also raises the question of whether the *trans*-cleavage activity of Cas12a on G4 is possible *in vivo* since G4s widely exist in organism genomes.[9,29]

In summary, we herein report that activated LbCas12a has *trans*-cleavage activity on DNA G4. We anticipate that this new finding will be further explored for more biochemical applications.

We gratefully acknowledge the financial support from the National Key R&D Program of China (2016YFA0501201 and 2018YFE0202300), the National Natural Science Foundation of China (21904139, 21735007, 21991081, and 21921004), and CAS Pioneer Hundred Talents Program (Y9Y1041001).

Conflicts of interest

There are no conflicts to declare.

Notes and references

1 B. Zetsche, J. S. Gootenberg, O. O. Abudayyeh, I. M. Slaymaker, K. S. Makarova, P. Essletzbichler, S. E. Volz, J. Joung, J. van der Oost, A. Regev, E. V. Koonin and F. Zhang, *Cell*, 2015, **163**, 759–771.
2 I. Fonfara, H. Richter, M. Bratovič, A. Le Rhun and E. Charpentier, *Nature*, 2016, **532**, 517–521.
3 P. Samai, N. Pyenson, W. Jiang, G. W. Goldberg, A. Hatoum-Aslan and L. A. Marraffini, *Cell*, 2015, **161**, 1164–1174.
4 A. V. Wright, J. K. Nunez and J. A. Doudna, *Cell*, 2016, **164**, 29–44.
5 J. S. Chen, E. Ma, L. B. Harrington, M. Da Costa, X. Tian, J. M. Palefsky and J. A. Doudna, *Science*, 2018, **360**, 436–439.
6 S.-Y. Li, Q.-X. Cheng, J.-K. Liu, X.-Q. Nie, G.-P. Zhao and J. Wang, *Cell Res.*, 2018, **28**, 491–493.
7 J. P. Broughton, X. Deng, G. Yu, C. L. Fasching, V. Servellita, J. Singh, X. Miao, J. A. Streithorst, A. Granados, A. Sotomayor-Gonzalez, K. Zorn, A. Gopez, E. Hsu, W. Gu, S. Miller, C.-Y. Pan, H. Guevara, D. A. Wadford, J. S. Chen and C. Y. Chiu, *Nat. Biotechnol.*, 2020, 870–874, DOI: 10.1038/s41587-020-0513-4,.
8 J. S. Gootenberg, O. O. Abudayyeh, M. J. Kellner, J. Joung, J. J. Collins and F. Zhang, *Science*, 2018, **360**, 439–444.
9 J. Spiegel, S. Adhikari and S. Balasubramanian, *Trends Chem.*, 2020, **2**, 123–136.
10 Y. Li, C. Liu, X. Feng, Y. Xu and B. F. Liu, *Anal. Chem.*, 2014, **86**, 4333–4339.
11 K. W. Lim, V. C. M. Ng, N. Martín-Pintado, B. Heddi and A. T. Phan, *Nucleic Acids Res.*, 2013, **41**, 10556–10562.
12 E. Demkovicova, L. Bauer, P. Krafcikova, K. Tluckova, P. Tothova, A. Halaganova, E. Valusova and V. Viglasky, *J. Nucleic Acids*, 2017, **2017**, 9170371.
13 Y. Xue, Z. Y. Kan, Q. Wang, Y. Yao, J. Liu, Y. H. Hao and Z. Tan, *J. Am. Chem. Soc.*, 2007, **129**, 11185–11191.
14 Y. Wang and D. J. Patel, *Structure*, 1993, **1**, 263–282.
15 K. N. Luu, A. T. Phan, V. Kuryavyi, L. Lacroix and D. J. Patel, *J. Am. Chem. Soc.*, 2006, **128**, 9963–9970.
16 V. Limongelli, S. De Tito, L. Cerofolini, M. Fragai, B. Pagano, R. Trotta, S. Cosconati, L. Marinelli, E. Novellino, I. Bertini, A. Randazzo, C. Luchinat and M. Parrinello, *Angew. Chem., Int. Ed.*, 2013, **52**, 2269–2273.
17 H. X. Jiang, Y. Cui, T. Zhao, H. W. Fu, D. Koirala, J. A. Punnoose, D. M. Kong and H. Mao, *Sci. Rep.*, 2015, **5**, 9255.
18 A. Wlodarczyk, P. Grzybowski, A. Patkowski and A. Dobek, *J. Phys. Chem. B*, 2005, **109**, 3594–3605.
19 J. B. Chaires, *FEBS J.*, 2010, **277**, 1098–1106.
20 E. Largy, J. L. Mergny and V. Gabelica, *Role of Alkali Metal Ions in G-Quadruplex Nucleic Acid Structure and Stability*, Springer Verlag, Germany, 2016, vol. 16, pp. 203–258.
21 T. Swartjes, R. H. J. Staals and J. van der Oost, *Biochem. Soc. Trans.*, 2020, **48**, 207–219.
22 Y. Dai, R. A. Somoza, L. Wang, J. F. Welter, Y. Li, A. I. Caplan and C. C. Liu, *Angew. Chem., Int. Ed.*, 2019, **58**, 17399–17405.
23 L. Lv, Z. Guo, J. Wang and E. Wang, *Curr. Pharm. Des.*, 2012, **18**, 2076–2095.
24 B. Ruttkay-Nedecky, J. Kudr, L. Nejdl, D. Maskova, R. Kizek and V. Adam, *Molecules*, 2013, **18**, 14760–14779.
25 J. Ida, S. K. Chan, J. Glökler, Y. Y. Lim, Y. S. Choong and T. S. Lim, *Molecules*, 2019, **24**, 1079.
26 J. S. Gootenberg, O. O. Abudayyeh, J. W. Lee, P. Essletzbichler, A. J. Dy, J. Joung, V. Verdine, N. Donghia, N. M. Daringer, C. A. Freije, C. Myhrvold, R. P. Bhattacharyya, J. Livny, A. Regev, E. V. Koonin, D. T. Hung, P. C. Sabeti, J. J. Collins and F. Zhang, *Science*, 2017, **356**, 438–442.
27 D. Koirala, T. Mashimo, Y. Sannohe, Z. Yu, H. Mao and H. Sugiyama, *Chem. Commun.*, 2012, **48**, 2006–2008.
28 P. Chen, J. Zhou, Y. Wan, H. Liu, Y. Li, Z. Liu, H. Wang, J. Lei, K. Zhao, Y. Zhang, Y. Wang, X. Zhang and L. Yin, *Genome Biol.*, 2020, **21**, 78.
29 V. S. Chambers, G. Marsico, J. M. Boutell, M. Di Antonio, G. P. Smith and S. Balasubramanian, *Nat. Biotechnol.*, 2015, **33**, 877–881.